The Effects of Temperature, Radiation, and Illumination on Current–Voltage Characteristics of Au/PVA(Co, Zn-Doped)/n-Si Schottky Diodes

İlbilge Dökme,[1] Şemsettin Altindal,[2] İbrahim Uslu[1]

[1]*Science Education Department, Faculty of Gazi Education, Gazi University, Ankara, Turkey*
[2]*Physics Department, Faculty of Arts and Sciences, Gazi University, Teknikokullar, Ankara 06500, Turkey*

Received 29 July 2011; accepted 16 September 2011
DOI 10.1002/app.36327
Published online 6 January 2012 in Wiley Online Library (wileyonlinelibrary.com).

ABSTRACT: Polyvinyl alcohol (PVA)/(Co-Ni) nanofiber film was fabricated on silicon wafer using electrospinning technique. The topography of the produced PVA/(Co-Ni) nanofiber film was examined by scanning electron microscopy (SEM). The Au/Poly (vinyl alcohol) (Co, Ni-doped)/n-Si Schottky diode (SD) was thermally formed in evaporating system after the spinning process. At first, the current–voltage (*I–V*) characteristics of Au/PVA (Co, Zn-doped)/n-Si SD was measured at the room temperature (300 K). For the investigating the effect of temperature, illumination and radiation on Au/PVA (Co, Zn-doped)/n-Si SD comparatively, the measurement was performed under the illumination intensity of 200 W, at 380K, and finally the radiation dose of 22 kGy respectively. The diode characteristics such as the zero-bias barrier height (Φ_{Bo}), ideality factor (n) and series resistance (R_s) were calculated at room temperature and under the condition of high temperature, illumination, and radiation. It was found that these characteristics were affected by the illumination and radiation as well as the temperature. The density of interface states (N_{ss}) distribution profiles as a function of (E_c - E_{ss}) extracted from the forward *I–V* measurements were also affected by illumination and radiation even if just a bit. © 2012 Wiley Periodicals, Inc. J Appl Polym Sci 125: 1185–1192, 2012

Key words: Au/PVA(Co,Zn-doped)/n-Si; nanofier; Schottky diode; polyvinyl alcohol; electrospinning technique

INTRODUCTION

Polyvinyl alcohol (PVA) has excellent film forming, emulsifying, and adhesive properties with a melting point of 230°C and 180–190°C for the fully hydrolyzed and partially hydrolyzed grades, respectively. It is a good insulating material with low conductivity and hence is of importance to microelectronic and optoelectronic application.[1,2] A metal such as bor (B), nickel (Ni), and zinc (Zn) doping PVA films causes improvement of the polymer behavior and often even brings about a progress in performance.[3] Therefore, PVA doped a metal has become preferable materials to fabricate Schottky barrier diodes (SBDs) and solar cells especially in recent studies.[4,5] The performance of SBDs and solar cells is drastically influenced by the structural and external effects. In general, considering the performance of these devices, there are several structural effects that cause deviations of the ideal behavior, and, therefore, they must be taken into account. These include the effects of interfacial layer, interface states (N_{ss}), and the barrier homogeneity at metal/semiconductor (M/S) interface, series resistance (R_s) of device, and fabrication process. However, studying the effect of external parameters such as radiation, illumination, and temperature has been of interest, especially the physical properties of semiconductor devices for the future research on satellite communication.

The electrical characteristics of fabricated Au/PVA (x-doped)/n-Si SBDs as a function of temperature or illumination/radiation were reported separately in our previous studies.[4–13] In this study, however, the effect of temperature, illumination, and radiation on the structural parameters of Au/PVA (Co, Zn-doped)/n-Si comparatively analyzed with synthesize the previous studies in the aggregate of the external parameters.

EXPERIMENTAL PROCEDURE

The schematic cross-section of the fabricated Au/PVA (Co, Zn-doped)/n-Si Schottky devices is seen in Figure 1. The detail of fabricated and measurements procedure is explained step by step in following section.

Forming ohmic back contact

The semiconductor used in this study was n-type (phosphor doped) single crystal silicon (111) with a thickness of 350 μm, and a resistivity of 0.7 Ω-cm.

Correspondence to: İ. Dökme (ilbilgedokme@gazi.edu.tr).

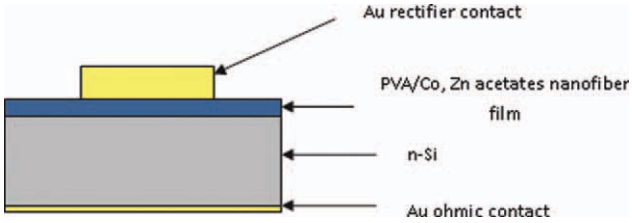

Figure 1 Schematic cross-section of the fabricated device. [Color figure can be viewed in the online issue, which is available at wileyonlinelibrary.com.]

For the initial fabrication process, Si wafer was degreased in organic solution of peroxide- ammoniac solution in 10 min and then etched in a sequence of H_2O + HCl solution and finally quenched in deionized water for a prolonged time. Preceding each cleaning step, the wafer was rinsed thoroughly in deionized water of resistivity of 18 M Ω cm. Immediately, after surface cleaning, high purity (99.999%) gold with a thickness of ~ 2000 Å was thermally evaporated from the tungsten filament onto the whole backside of half wafer at a pressure of $\sim 2 \times 10^{-6}$ Torr in oil vacuum pump system. The ohmic contacts were prepared by sintering the evaporated Au back contact at 450°C for 5 min in flowing dry nitrogen ambient at rate of 2 L/min.

Preparation of PVA/Co, Zn and spinning PVA/Co, Zn on Si wafer

0.5 grams of cobalt acetate and 0.25 g of zinc acetate was mixed with 1 g of PVA, molecular weight = 72,000 and 9 mL of deionized water. After vigorous stirring for 2 h at 50°C, a viscous solution of PVA (Co, Zn-doped) was obtained. The conductivity of PVA (Co, Zn-doped) polymer was measured 1.21×10^{-6} S cm^{-1} using four point probe technique (ENTEK Company). The solution of the PVA (Co, Zn-doped) was homogenized for 1.5 h by mixing with rotation before the deposition. PVA (Co, Zn-doped) nanofiber film on n-Si substrate was coated by electrospinning technique. Electrospinning process utilizes electrical force to produce polymer fibers. The composite solution for spinning was loaded into a 10 mL hypodermic stainless steel syringe with a needle (0.8-mm diameter and 38-mm length) connected to a digitally controlled pump (New Era) which provides a constant feeding rate. The positive electrode of a high-voltage power supply (SP-30P) was placed on to the top of the needle. The negative electrode was connected to a metallic stationary collector wrapped with aluminum foil and served as a counter electrode and spun under 20 kV. The working distance between the tip of the syringe needle and the collector was 19.5 cm. Composite fibers were collected on Si wafer on the aluminum foil, dried at 60°C under vacuum for 10 h. The solvent evaporated and a charged fiber was deposited onto the Si wafer as a non-woven mat. The fibers thus formed were dried in vacuum for 12 h at 80°C. Fiber formation and morphology of the electrospun PVA/Co, Ni acetate fibers determined using a scanning electron microscope (SEM) Quanto 400 FEI MK-2 are given in Figure 2.

Fabricating Schottky/rectifier contact and capacitance–conductance measurements

After spinning process, Au circular rectifier contacts were coated by evaporation with a diameter of about 1.0 mm (diode area = $7.85 \times 10^{-3} cm^2$). Figure 1 shows the typical device structure used in this work. The forward and reverse bias *I–V* measurements were performed by the use of a Keithley 2400 source meter at the temperature of 300 and 380 K using a temperature-controlled Janis vpf-475 cryostat, which enabled us to make measurements in the temperature range of 77–450 K. For illuminating the sample, a 200 W solar simulator (Model: 69931, Newport-Oriel Instruments, Stratford, CT) was used as a light source. The photons at different power levels passed through an AM1.5 filter which allows wavelengths only between 400 and 700 nm, and reaches the surface of the devices. The intensity of the light was measured by research radiometer (Model ILT1700, International Light Technologies, MA). The *I–V* measurements were finally performed before and after ^{60}Co γ-ray source irradiation with the dose rate of 22 kGy/h at room temperature.

RESULTS AND DISCUSSION

For a Schottky structure with the series resistance and the ideality factor greater than unity, the current–voltage

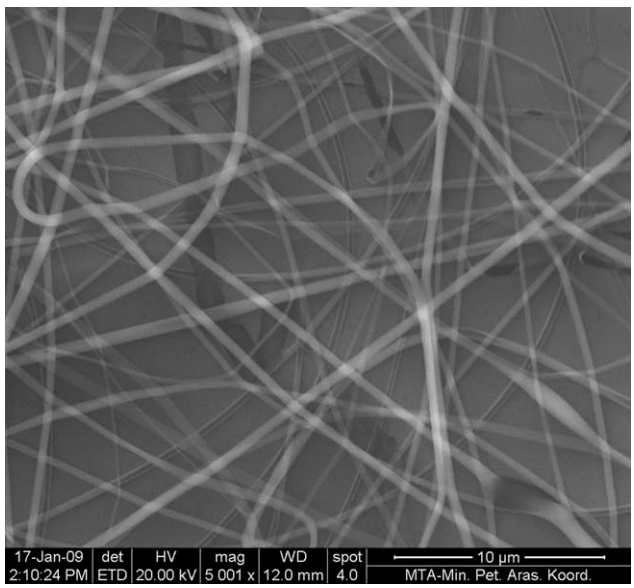

Figure 2 SEM images of PVA (Co, Zn, acetates) nanofibers.

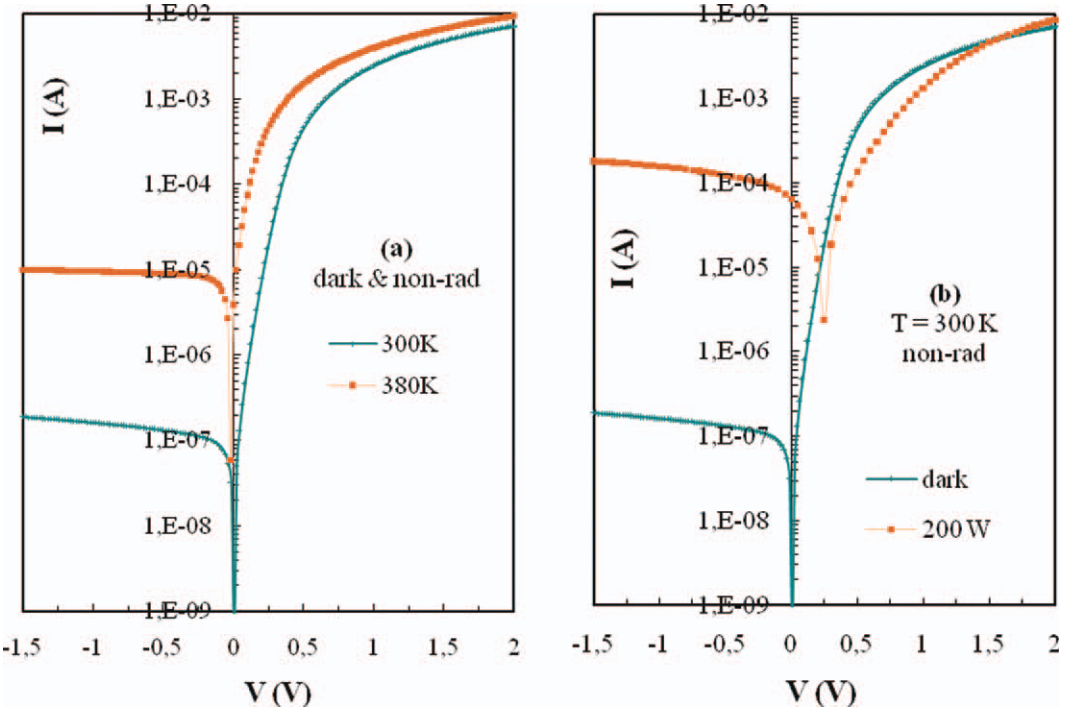

Figure 3 The experimental semilogarithmic *I–V* characteristics of the Au/PVA (Co, Zn-doped)/n-Si SD (a) at 300 and 380 K, (b) before and after radiation dose of 22 kGy, (c) in dark and under illumination intensity of 200 W. [Color figure can be viewed in the online issue, which is available at wileyonlinelibrary.com.]

relation based on thermionic emission (TE) theory can be expressed as[14–17]

$$I = I_o\left[\exp\frac{q}{nkT}(V - IR_s)\right] \tag{1a}$$

where V is the definite forward bias voltage, IR_s term is the voltage drop across series resistance of the device, n is the ideality factor, k is the Boltzmann constant, and T is temperature in Kelvin, and I_o is the reverse saturation current. The value of I_o can be obtained from the y-axis intercept of the linear region of the semi-log-forward bias *I–V* plots and expressed as

$$I_o = A^{\times} A\ T^2\ \exp(-q\Phi_{Bo}\ /kT) \tag{1b}$$

where the quantities A^*, A, Φ_{Bo} are the effective Richardson constant and equals to 120 A/cm^2 K^2 for n-type Si, the diode area and, the zero-bias barrier height, respectively.

Ideality factor is a measure of conformity of the diode to pure TE and is contained in the slope of straight line region of the forward bias logarithmic characteristics of *I–V* plot through the relation[15]

$$n = \frac{q}{kT}\left[\frac{d(V)}{dLn(I)}\right] \tag{2}$$

The experimental semi-logarithmic *I–V* characteristics of the Au/PVA (Co, Zn-doped)/n-Si Schottky diode (SD) at 300 and 380K, before and after radiation dose of 22 kGy and, in dark and under illumination intensity of 200 W are shown Figure 3(a–c), respectively. The Φ_{Bo} and n values of Au/PVA (Co, Zn-doped)/n-Si SD were calculated with the help of eqs. (1b) and (2) from the y-axis intercept and slope of the linear region of the semi-log-forward bias *I–V* plots, respectively These results are in Figures 4 and 5 and Table I.

As can be seen in Table I and Figures 4 and 5, the diode parameters of n and Φ_{Bo} are influenced by temperature, radiation and illumination. The value of n calculated *I–V* characteristics decreases with increasing temperature, however, decreasing illumination and radiation. An increase in temperature provides positive impact on ideality factor, but an increase in illumination and radiation provide negative impact on it. The values of zero-bias barrier height of Au/PVA (Co, Zn-doped)/n-Si SD were found 0.75 eV (at 300 K) and 0.82 eV (at 380 K) from Eq. (1b) under the condition of controlling other effect (radiation and illumination). While the ideality factor decreases with increasing temperature from 300 K to 380 K, the zero-bias barrier height increases with increasing temperature from 300 K to 380 K. As can be reviewed in the literature,[18–23] the negative temperature coefficient of Φ_{Bo} conflicting TE has been reported. The nature of eqs. (1a,b) principally require the negative temperature coefficient of Φ_{Bo}. The illumination intensity of 200 W causes an increase in

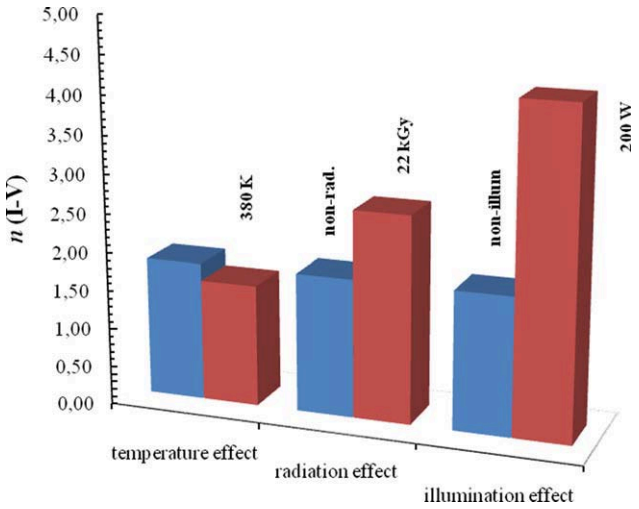

Figure 4 Temperature, radiation, and illumination effect on the ideality factor of the Au/PVA (Co, Zn-doped)/n-Si SD. [Color figure can be viewed in the online issue, which is available at wileyonlinelibrary.com.]

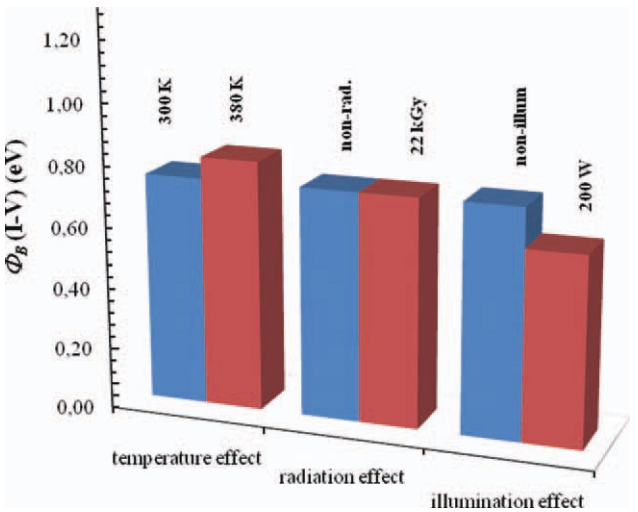

Figure 5 Temperature, radiation, and illumination effect on zero-bias barrier height of the Au/PVA (Co, Zn-doped)/n-Si SD. [Color figure can be viewed in the online issue, which is available at wileyonlinelibrary.com.]

ideality factor, but decrease in Φ_{Bo}. However, there is no effect of the radiation dose of 22 kGy on the diode parameters of zero-bias barrier height.

The amount of n greater than unity arises from the variation of barrier height with applied voltage, which leads to extra current mechanism such as thermionic-field emission, generation-recombination, tunneling.[24–27]

However, the lightly doped semiconductors generally requiring SDs offer series resistance (R_s) and so a significant voltage drop occurs across that at large forward bias region. Therefore, the forward bias semi-logarithmic I–V characteristic deviates considerably from linearity due to the effect of series resistance R_s, interfacial layer and the interface states when the applied voltage is sufficiently large.[15] The series resistance is important in the downward concave curvature of the forward bias I–V characteristics, while the other two parameters are important in both linear and nonlinear regions of I–V characteristics. Therefore, the ideality factor, the barrier height, and the series resistance can be evaluated using a method developed by Cheung and Cheung[28] in the high current range where the I–V characteristic is not linear. According to this method from eq. (1a), the following functions can be written as

$$\frac{dV}{dLnI} = n\frac{kT}{q} + IR_s \tag{3}$$

$$H(I) = V + n\frac{kT}{q}Ln\left(\frac{I}{AA^{\times}T^2}\right) \tag{4}$$

and $H(I)$ is given as follows:

$$H(I) = n\Phi_{B_o} + IR_s \tag{5}$$

The experimental $dV/d(\mathrm{Ln}I)$ versus I and $H(I)$ versus I plots of the Au/PVA (Co, Zn-doped)/n-Si SD at 300 and 380K (dark and nonradiation) are presented in Figures 6(a,b), respectively. Equation (3) should give a straight line for the data of downward curvature region in the forward bias I–V characteristic. Thus, a plot of $dV/d(\ln I)$ versus I will give R_s as the slope and nkT/q as the y-axis intercept. Using the n value determined from eq. (3) and the data of downward curvature region in eq. (4), a plot of $H(I)$

TABLE I
The Experimental Values of Diode Parameters Obtained from the Forward *I–V* Characteristics

Variables	Variables under control	n (I-V)	n ($dV/dLnI$)	Φ_{Bo} (I-V) (eV)	Φ_{Bo} ($H(I)$) (eV)	R ($dV/$dL nI) (Ω)	$R_s(H(I))$ (Ω)
300 K	nonnon-illumination non-radiation	1.80	1.74	0.75	0.75	276.11	263.07
380 K	nonnon-illumination non-radiation	1.58	1.40	0.82	0.80	211.20	185.56
Radiation dose of 22 kGy	Temperature (300 K) non-illumination	2.68	2.12	0.75	0.95	218.02	215.24
Illumination intensity of 200 W	Temperature (300 K) nonradiation	4.20	3.89	0.62	0.56	116.14	118.89

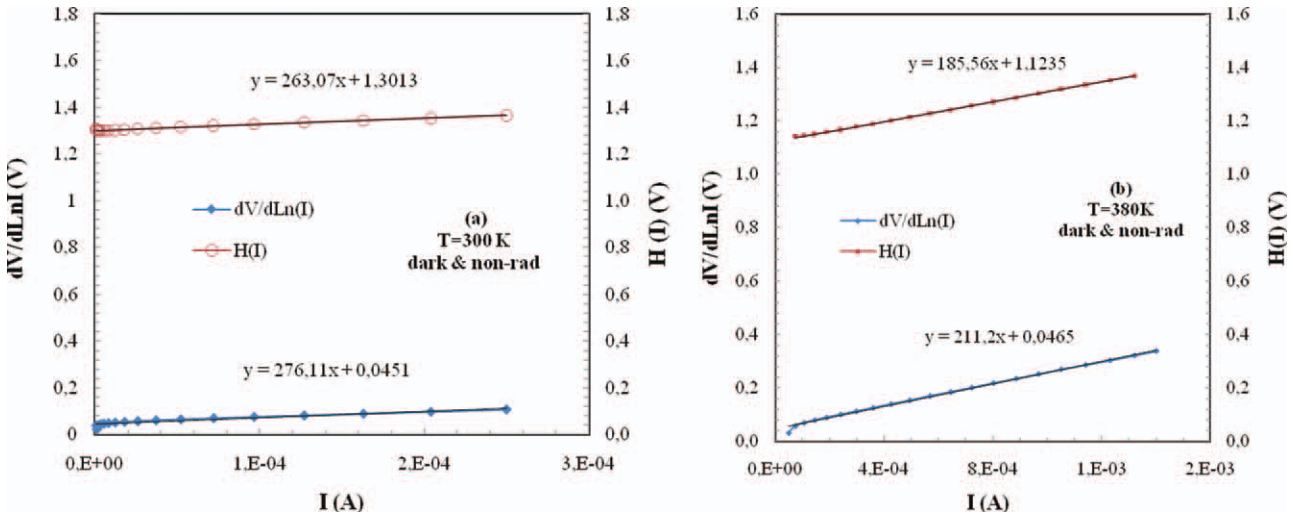

Figure 6 The $dV/d\ ln\ (I)$ versus I and $H(I)$ versus I plots of the Au/PVA (Co, Zn-doped)/n-Si SD (a) at 300 (in dark & nonradiation) and (b) 380 K (in dark & nonradiation). [Color figure can be viewed in the online issue, which is available at wileyonlinelibrary.com.]

versus I according to eq. (5) will also give a straight line with y-axis intercept equal to $n\Phi_{Bo}$.

From $dV/d(\ln I)$ versus I plot by means of eq. (3), the values of R_s and n of Au/PVA (Co, Zn-doped)/n-Si SD at 300 and 380 K under condition of nonradiation and dark are given in Table I. The values of Φ_{Bo} and R_s from $H(I)$–I plot according to eq. (5) are also seen in this table.

The experimental $dV/d(\ln I)$ versus I and $H(I)$ versus I plots of the Au/PVA (Co, Zn-doped)/n-Si SD in radiation dose of 22 kGy and under illumination intensity of 200 W are shown in Figure 7(a,b), respectively. The values of R_s and n and Φ_{Bo} of Au/PVA (Co, Zn-doped)/n-Si SD in radiation dose of 22 kGy and under illumination intensity of 200 mW/cm^2 at 300 K are given in Table I. As can been in Table I and Figures 6 and 7, since the linear range of the forward I–V plots is reduced, the values of n calculated from TE theory are poorer than those calculated from Cheung function. The obtained Φ_{Bo} values by TE and $H(I)$ function are in good agreement with each other. The R_s values calculated from eqs. (3) and (5) are close. The decrease in series resistance with an increasing temperature is usual behavior for semiconductors. Such temperature dependence of R_s is an obvious agreement with the reported negative temperature coefficient of the R_s.[29,30] However, the detail of the effect of radiation and the illumination on electrical characteristics of these devices is unclear.

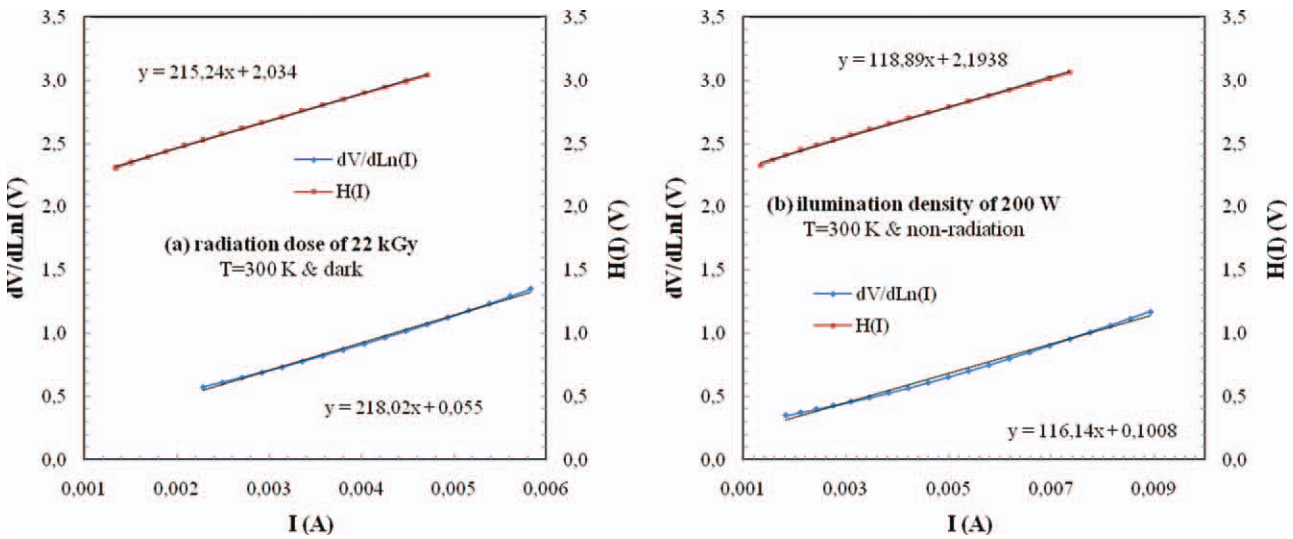

Figure 7 The $dV/d\ ln\ (I)$ versus I and $H(I)$ versus I plots of the Au/PVA (Co, Zn-doped)/n-Si SD (a) under the radiation dose of 22 kGy (in the condition of dark and at 300 K) and (b) under the illumination intensity of 200 W (in the condition of nonradiation and at 300 K). [Color figure can be viewed in the online issue, which is available at wileyonlinelibrary.com.]

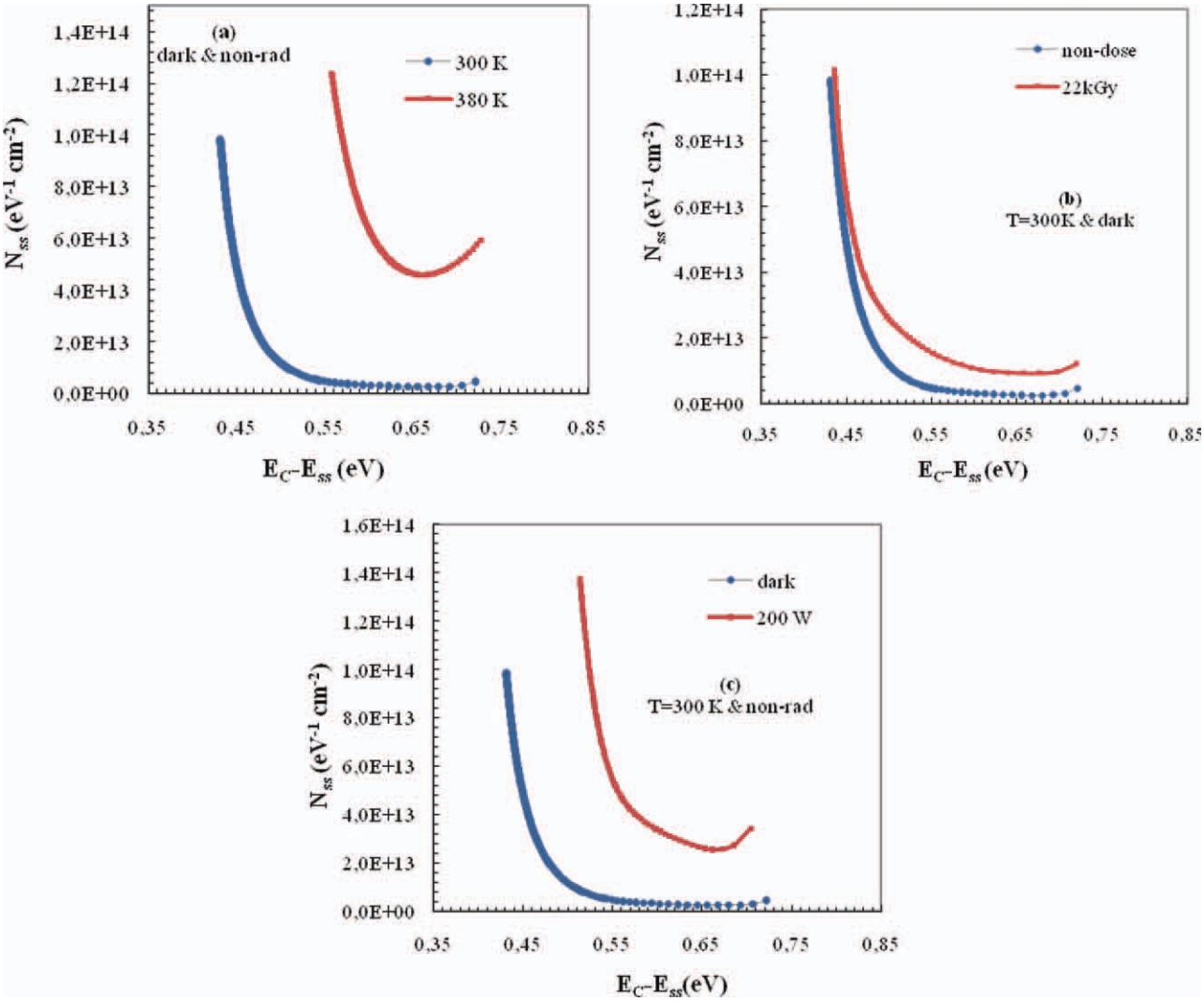

Figure 8 The interface states energy distribution curves of Au/PVA (Co, Zn-doped)/n-Si SD Under condition of (a) 300 K and dark, (b) nonradiation and dark, and (c) 300 K and nonradiation. [Color figure can be viewed in the online issue, which is available at wileyonlinelibrary.com.]

The results on interface states reported literature indicated that the interface states density (N_{ss}) is also important effect for high value of ideality factor.[31,32] The sufficiently thick interface layer disconnects the interface states from the metal, making them communicate with the semiconductor more readily than with the metal. Less information exists about interface states in organic materials for Schottky structure. Stallinga et al.[33] and Berleb et al.[34] use admittance spectroscopy to find evidence for trapped charge at an organic–organic interface, but no information was found as to the distribution of these charges in energy. Here, we obtained the energy density distribution profile of interface states from the forward *I–V* characteristics of the Au/PVA (Co, Zn-doped)/n-Si SD.[35] Since the values of ideality factor and barrier height are assumed to be voltage dependent, for a Schottky structure with interface states governed by the semiconductor, the expression for the density of interface states as deduced by Card and Rhoderick[35] can be written as following equations:

$$n(V) = \frac{q}{kT}\left[\frac{V}{Ln(I/I_o)}\right] \tag{6a}$$

$$\Phi_e = \Phi_{Bo} + \beta(V) = \Phi_{Bo} + (1 - \frac{1}{n(V)})V \tag{6b}$$

$$N_{ss}(V) = \frac{1}{q}\left[\frac{\varepsilon_i}{\delta}(n(V) - 1) - \frac{\varepsilon_s}{W_D}\right] \tag{6c}$$

where β is the voltage coefficient of the effective barrier height Φ_e, δ is the thickness of interfacial layer calculated eq. (10) in Ref. [34], W_D is the width of the space charge region (obtained from the experimental C^{-2} versus V plots at 500 kHz), ε_i and ε_s are permittivity of the interfacial insulator layer and the semiconductor, respectively, and N_{ss} is the density of the

interface states in equilibrium with the semiconductor, respectively.

The energy of the interface states E_{ss} (for *n*-type semiconductors) with respect to the bottom of the conduction band at the surface of semiconductor is given by[24–27,36]

$$E_c - E_{ss} = q(\Phi_e - V) \quad (7)$$

Figure 8(a–c) show the energy distribution profile of the N_{ss} obtained from the forward bias *I–V* characteristics of the Au/PVA (Co, Zn-doped)/n-Si SD at 300 and 380 K, before and after radiation dose of 22 kGy and, in dark and under illumination intensity of 200 W, respectively. The results from Figure 8 can be specified as follows:

1. Under condition of nonradiation and dark, the energy values of the density distribution of Au/PVA (Co, Zn-doped)/n-Si SD are in the range (E_c − 0.43) to (E_c − 0.72) eV at 300 K. The values of the N_{ss} at 300 K in (E_c − 0.43) and (E_c − 0.72) are 9.65 × 10^{13} and 4.63 × 10^{12} eV^{-1} cm^{-2}, respectively.
2. Under condition of nonradiation and dark, the energy values of the density distribution of Au/PVA (Co, Zn-doped)/n-Si SD are in the range (E_c − 0.55) to (E_c − 0.72) eV at 380 K. The values of the N_{ss} at 380 K in (E_c − 0.55) and (E_c − 0.72) are also 1.21 × 10^{14} and 5.94 × 10^{13} eV^{-1} cm^{-2}, respectively.
3. Under condition of 300 K and dark, the energy values of the density distribution of Au/PVA (Co, Zn-doped)/n-Si SD are in the range (E_c − 0.44) to (E_c − 0.72) eV at 22 kGy. The values of the N_{ss} at (22 kGy) in (E_c − 0.44) and (E_c − 0.72) are also 1.00 × 10^{14} and 1.21 × 10^{13} eV^{-1} cm^{-2}, respectively.
4. Under condition of 300 K and nonradiation, the energy values of the density distribution of Au/PVA (Co, Zn-doped)/n-Si SD are in the range (E_c − 0.51) to (E_c − 0.70) eV under the illumination intensity of 200 W. The values of the N_{ss} (under the illumination intensity of 200 W) in (E_c − 0.51) and (E_c − 0.70) are also 1.36 × 10^{14} and 3.44 × 10^{13} eV^{-1} cm^{-2}, respectively.

As can be seen all these results, the exponential growth of the N_{ss} from midgap toward the bottom of conduction band is very apparent.[43]

CONCLUSION

The Au/Poly (vinyl alcohol) (Co, Ni-doped)/n-Si SD was fabricated. The measurement of *I–V* characteristics were performed 380 K, under illumination intensity of 200 W and radiation dose of 22 kGy. The main diode characteristics of ideality factor decreased with the effect of increasing temperature. However, it increased with the effect of increasing illumination and radiation. While barrier height decreased with an increase in illumination intensity in proportion to dark, it was seen an increase in barrier height with increasing temperature. Such an effect of the temperature on *n* and Φ_{Bo} results from the nature of the TE. However, the detail of the effect of radiation and the illumination on electrical characteristics of Au/PVA (Co, Ni-doped)/n-Si SD is unclear. Being exposing to radiation or illumination may be cause the change in the equilibrium of interface states. The density of interface states (N_{ss}) distribution profiles of Au/PVA (Co, Ni-doped)/n-Si as a function of (E_c - E_{ss}) were influenced by the temperature, illumination. The values of N_{ss} (in 0.65 V) were found to be ≈2.61 × 1012 $cm^{-2}eV^{-1}$ at 300 K, ≈4.5 × 1013 $cm^{-2}eV^{-1}$ at 380 K, ≈9.33 × 1012 $cm^{-2}eV^{-1}$ under 22 kGy dose of radiation and ≈2.62 × 1013 $cm^{-2}eV^{-1}$ under illumination intensity of 200 W. All the results indicate that the effects of illumination and radiation on Schottky device with polymeric interfacial layer are considerably important as well as the temperature effect.

References

1. Abdel-Malik, T. G.; Abdel-Latif, R. M.; Sawaby, A.; Ahmed, S. M. J Appl Sci Res 2010, 4, 331.
2. Shinha, H. C.; Talwar, I. M.; Srivasta, A. P. Thin Solid Films,1989, 82, 229.
3. Ahmed, M. A.; Abo-Ellil, M. S. J Mater Sci Mater Electronics 1998, 9, 391.
4. Tunç, T.; Altindal, Ş.; Uslu, I.; Dökme, I.; Uslu, H. Mater Sci Semicond Process,2011, 14, 139.
5. Uslu, H.; Altindal, Ş.; Tunç, T.; Uslu, I.; Mammadov, T. S. J Appl Polym Sci 2011, 120, 322.
6. Altindal, Ş; Uslu, H. J Appl Phys 2011, 109, 074503.
7. Uslu, H.; Altindal, Ş.; Dökme, I. J Appl Phys 2010, 108, 104501.
8. Taşçioglu, I.; Uslu, H.; Altindal, Ş.; Durmuş, P.; Dökme, I.; Tunç, T. J Appl Polym Sci,2010, 118, 596.
9. Tunç, T.; Altindal, Ş.; Dökme, I.; Uslu, H. J Electron Mater,2011, 40, 157.
10. Taşçioglu, I.; Aydemir, U.; Altindal, Ş. J Appl Phys 2010, 108, 064506.
11. Dökme, I.; Altindal, Ş.; Tunç, T.; Uslu, I. Microelectron Reliab 2010, 50, 39.
12. Tunç, T.; Uslu, I.; Dökme, I.; Altindal, Ş.; Uslu, H. Int J Polym Sci 2010, 59, 739.
13. Dökme, I.; Tunç, T.; Uslu, I.; Altindal, Ş. Synth Met,2011, 161, 474.
14. Sze, S. M. Physics of Semiconductor Devices, 2nd ed.; Wiley: New York, 1981, p850.
15. Norde, H. J Appl Phys 1979, 50, 5052.
16. Cheung, S. K.; Cheung, N.W. Appl Phys Lett 1986, 49, 85.
17. Singh, A. Solid State Electron 1985, 28, 223.
18. Demircioglu, O.; Karataş, Ş.; Yildirim, N.; Bakkaloglu, O. F.; Türüt, A. J Alloy Compound,2011, 509, 6433.
19. Farag, A. A. M.; Yahia, I. S. Synth Met,2011, 161, 32.
20. Aydogan, Ş.; Incekara, U.; Deniz, A. R.; Türürt, A. Microelectron Eng 2010, 87, 2525.

21. Yildirim, N.; Ejderha, K.; Türüt, A. J Appl Phys, 2010, 108, 114506.
22. Ejderha, K.; Yildirim, N.; Türüt, A.; Abay, B. Süperlattices and Microstructures,2010, 47, 241.
23. Çinar, K.; Yildirim, N.; Coşkun, C.; Türüt, A. J Appl Phys 2009, 106, 073717.
24. Singh, A.; Reinhardt, K. C.; Anderson, W. A. J Appl Phys 1990, 68, 3475.
25. Cova, P.; Singh, A. Solid State Electron 1990, 33, 11.
26. Singh, A. Solid State Electron,1985, 28, 223.
27. Altindal, Ş.; Dökme, I.; Bülbül, M.; Yalçin, N.; Serin, T. Microelectron Eng 2006, 83, 499.
28. Cheung, S. K.; Cheung, N. W. Appl Phys Lett 1986, 49, 85.
29. Osvald, J.; Horvath, Zs. J. Appl Surf Sci 2004, 234, 349.
30. Horvath, Zs. J.; Adam, M.; Pinter, I.; Cvikl, B.; Korosak, D.; Mrdjen, T.; Tuyen, V. V.; Makaro, Zs.; Ducso, Cs.; Barsony, I. Vacuum 1998, 50, 385.
31. Aydin, M. E.; Yakuphanoglu, F.; Eom, J.; Hwang, D. Phys B 2007, 387, 239.
32. Yakuphanoglu, F. J Phys Chem C 2007, 111, 1505.
33. Stallinga, P.; Gomes, H. L.; Murgia, M.; Müllen, K. Org Electron 2002, 3, 43.
34. Berleb, S.; Brütting, W.; Paasch, G. Org Electron 2000, 1, 41.
35. Card, H. C.; Rhoderick, E. H. J Phys D Appl Phys 1971, 4, 1589.
36. Güllü, Ö.; Aydogan, Ş.; Türüt, A. Microelecron Eng 2008, 85, 1647.